ONLINE FIRST

This is a provisional PDF only. Copyedited and fully formatted version will be made available soon.

POLISH GYNECOLOGY
GINEKOLOGIA POLSKA
ORGAN POLSKIEGO TOWARZYSTWA GINEKOLOGICZNEGO
THE OFFICIAL JOURNAL OF THE POLISH GYNECOLOGICAL SOCIETY

ISSN: 0017-0011

e-ISSN: 2543-6767

Integrated analysis identified novel miRNAs and mRNA in endometriosis

Authors: He Ma, Xueqin Sun, Yanlin Wang, Hongcheng Tian, Kaixue Lao, Jingjing Yan, Xinghua Diao

DOI: 10.5603/GP.a2022.0078

Article type: Research paper

Submitted: 2021-09-27

Accepted: 2022-06-17

Published online: 2022-09-26

ORIGINAL PAPER / GYNECOLOGY

Integrated analysis identified novel miRNAs and mRNA in endometriosis

Short title: Deregulated microRNA and mRNA in endometriosis

He Ma[1], Xueqin Sun[2], Yanlin Wang[1], Hongcheng Tian[1], Kaixue Lao[1], Jingjing Yan[3], Xinghua Diao[1]

[1]*Department of Reproductive Medicine, Binzhou Medical University Hospital, China*
[2]*Department of Gynecology, Zibo Central Hospital, China*
[3]*Department of Clinical Laboratory, Binzhou Medical University Hospital, China*

Corresponding author:
Xinghua Diao
Department of Reproductive Medicine, Binzhou Medical University Hospital, No. 661, Huanghe 2 Road, Binzhou, Shandong 256600, China
phone: + 86-15905431066
e-mail: sddiaoxh@126.com

ABSTRACT

Objectives: Endometriosis is a common gynecological disease that seriously affects women's health and quality of life. However, the pathogenesis of endometriosis remains uncertain. This study aims to find the key microRNAs (miRNAs) and mRNAs and further to elucidate the pathogenesis of endometriosis.

Material and methods: Differentially expressed mRNAs (DEmRNAs) and the differentially expressed miRNAs (DEmiRNAs) were obtained by Gene Expression Omnibus (GEO) datasets integration analysis. Functional enrichment analysis of DEmRNAs and DEmRNAs targeted by DEmiRNAs was enforced using GeneCodis3. The DEmiRNA-DEmRNA interaction network was built using Cytoscape. The expression of candidate DEmRNA and DEmiRNA was verified using quantitative real

time-polymerase chain reaction (QRT-PCR) and online datasets followed by diagnostic and immune cell infiltration analysis.

Results: A total of 835 (327 down-regulated and 508 up-regulated) DEmRNAs and 39 (24 down-regulated and 15 up-regulated) DEmiRNAs were identified between ectopic endometria (EC) group and eutopic endometria (EU) group. DEmRNAs targeted by DEmiRNAs were markedly enriched in cell adhesion molecules, pathways in cancer, leukocyte transendothelial migration, cytokine-cytokine receptor interaction and MAPK signaling pathway. The DEmiRNA-DEmRNA interaction network of up-regulated miRNAs was consisted of 15 miRNAs and 188 corresponding mRNAs. For down-regulated miRNAs, the DEmiRNA-DEmRNA interaction network was consisted of 24 miRNAs and 305 corresponding mRNAs. QRT-PCR validation results of IRF6, PTGER3, NTRK2, hsa-miR-449a and hsa-miR-873-5p were in line with the GEO analysis result. RF6, PTGER3 and NTRK2 had a potential diagnostic value for endometriosis. In addition, the infiltration of macrophages M2 and NK cells activated was the most significantly increased and reduced in ectopic endometrial, respectively.

Conclusions: These identified DEmRNAs and DEmiRNAs may be may be associated with the pathogenesis of endometriosis. The integrated analysis of miRNA and mRNA expression profiles may provide a new perspective for understanding the mechanisms of endometriosis and developing new treatments.

Key words: endometriosis; microRNAs; Gene Expression Omnibus datasets; integrated analysis

INTRODUCTION

Endometriosis is a common occurring gynaecological disease characterised by estrogen-dependent chronic inflammatory process that mainly affects chronic pelvic pain, dysmenorrhea and infertility . At present, the main treatment strategies of endometriosis are surgical resection and hormone inhibition. However, due to many side effects and a high recurrence rate, there is no ideal treatment . The mechanism underlying endometriosis progression remains not fully understood. Thence, it is

crucial to reveal the underlying mechanism of endometriosis progression and to identify reliable molecular markers with diagnostic and therapeutic value for endometriosis.

Currently, with the advances of next-generation sequencing, especially microarray technology, a huge amount of data has been produced, among which the Gene Expression Omnibus (GEO) database is the largest comprehensive international public gene expression database . Gene expression microarray technology has been widely applied in the study of gene expression profile of multiple human diseases, which provide an effective approach for the study of disease-related genes and the discovery of new therapeutic targets and biomarkers . In recent years, some studies have reported the mRNA expression profile of endometriosis . However, due to small sample size, different data processing methods and sample heterogeneity, the results are inconsistent. Integrated bioinformatics analysis can overcome the shortcomings of these single studies and combine different microarray datasets to obtain more stable results . However, the key genes and signaling pathways in the progression of endometriosis remain unclear.

MicroRNAs (miRNAs) are a class of small non-coding RNA with 18–25 nucleotide RNAs, which mainly inhibits mRNA expression at the transcriptional level . In previous decades, miRNAs have been reported to be involved in many cellular processes, including proliferation and differentiation, and aberrant expression of miRNAs can also cause many diseases, including endometriosis . Although differences in miRNA expression profiles of endometriosis have been previously reported, few studies have focused on integrated analysis of miRNA-mRNA interactions. Herein, we evaluated the interaction between aberrant miRNAs and aberrant mRNAs in endometriosis, and built a network between them.

Objectives

The purpose of our study was to identify differentially expressed mRNAs (DEmRNAs) and differentially expressed miRNAs (DEmiRNAs) in endometriosis,

which might provide some candidate mRNAs and miRNAs for the treatment of endometriosis and provide a new theoretical basis for further experimental studies.

MATERIAL AND METHODS

Raw data collection

The miRNA/mRNA expression profiles in ectopic endometria (EC) and eutopic endometria (EU) tissue samples were downloaded from the GEO database with the keywords “endometriosis” and “Homo sapiens”. 4 mRNA datasets (GSE11691, GSE25628, GSE86534 and GSE105764) and 1 miRNA microarray dataset (GSE105765) were acquired. The GSE11691 series (GPL96 platform) included 19 (9 EC and 2 EU) specimens. The platform for GSE25628 was GPL571 including 6 EC and 7 EU samples. The platform for GSE86534, consisting of 4 EC and 4 EU samples, was GPL20115. GSE105764 included 8 EC and 8 EU tissue samples, and its platform was GPL20301. GSE105765 was in GPL11154 platform, which contained 8 EC and 8 EU tissue samples. The platform and serial matrix files were downloaded. The dataset information is listed in Table 1.

Differential expression analysis

Differential expression analysis of mRNAs was performed using the limma and metaMA package analysis. Inverse normal method was utilized to combine the p value. Benjamini and Hochberg method was used to analyze individual p values. The multiple comparison-corrected false discovery rate (FDR) was then obtained. The FDR < 0.05 and |Combined.ES| > 2 was considered as the cut-off criterion for DEmRNAs. To obtain DEmiRNAs between EC and EU tissue sample, the DESeq2 package in R was used for analysis with the cut-off criteria of FDR < 0.05 and | log2FC| > 3. The volcano map and hierarchical clustering analysis were produced using the R package.

Functional enrichment analysis

We used Gene Ontology (GO) and Kyoto Encyclopedia of Genes and Genomes

(KEGG) pathway enrichment analysis to uncover the biological functions of the DEmRNAs. The GeneCodis3 (http://genecodis.cnb.csic.es) was used for the GO enrichment and KEGG pathway enrichment analysis. The cut-off values for the significant of GO and KEGG terms was FDR < 0.05.

DEmiRNA-DEmRNA interaction analysis

The DEmiRNA-DEmRNA interaction pairs in EC vs EU were identified. First, six bioinformatic algorithms (RNA22, miRanda, miRDB, miRWalk, PICTAR2 and Targetscan) were utilized to predict the supposed target DEmRNAs of DEmiRNAs. Then, the DEmiRNA-DEmRNA pairs were recorded by ≥ 4 algorithms. Those DEmRNAs negatively correlated with DEmiRNAs were retained for further investigation. Ultimately, DEmiRNA-DEmRNA interaction networks were built by using Cytoscape 3.7.1 (http://www.cytoscape.org/).

Quantitative real time-polymerase chain reaction (QRT-PCR)

Four patients diagnosed as endometriosis and four normal controls were included in this study. This study has been approved by the ethics institute of Binzhou medical university hospital (2020-LW-025). The signed informed consent of all the participants was obtained. Total RNA was isolated using a TRIzol reagent (Invitrogen, USA). Complementary DNA reverse transcription and QRT-PCR were performed by Fast Quant RT Kit (Invitrogen, USA) and Super Real PreMix Plus SYBR Green (Invitrogen, Waltham, MA, USA), respectively. The human GAPDH and hsa-U6 was used as endogenous controls for mRNA and miRNA expression in analysis, respectively. The $2^{-\Delta\Delta Ct}$ method was used to process the data.

Expression validation and diagnostic analysis of DEmRNAs in online dataset

In order to further validate the expression of identified DEmRNAs, GSE7305 and GSE23339 datasets of endometriosis were used for expression analysis. In addition, diagnostic analysis of identified DEmRNAs was performed in the GSE23339 dataset.

Immune cell infiltration analysis in the tissue of endometriosis

The CIBERSORT algorithm (https://cibersort.stanford.edu/) was applied to estimate the burden of immune infiltration subtypes in the tissue of endometriosis, based on a linear support vector regression algorithm with mRNA expression data with systems-level mRNA expression data in the R toolkit.

RESULTS

DEmRNAs and DEmiRNAs in endometriosis

Four datasets (GSE11691, GSE25628, GSE86534 and GSE105764) were used to identify DEmRNAs according to the criteria of FDR < 0.05 and |Combined.ES| > 2. A total of 835 DEmRNAs were obtained between EC and EU, of which 508 mRNAs were up-regulated and 327 mRNAs down-regulated. Top ten up- and down-regulated DEmRNAs between EC and EU are listed in Table 2. Then, the volcano map of all DEmRNAs and the clustering heat map of the top 100 DEmRNAs were established, as presented in Figure 1A and Figure 1B, respectively. GSE105765 dataset was utilized to obtain DEmiRNAs with DESeq2 package in R. Under the threshold of FDR < 0.05 and |log2FC| > 3, 39 DEmiRNAs were identified, including 15 up-regulated and 24 down-regulated miRNAs. The all DEmiRNAs between EC and EU are listed in Table 3. Figure 1C and Figure 1D displayed the volcano map and heat map of all DEmiRNAs, respectively.

Functional enrichment analysis of DEmRNAs

As showed in Figure 2A, GO analysis results indicated that DEmRNAs were mainly enriched in signal transduction and multicellular organismal development in the biological process. In the cellular component analysis, DEmRNAs were primarily enriched in the cytoplasm and membrane. Molecular function analysis indicated that DEmRNAs mainly were enriched in protein binding, metal ion binding, nucleotide binding, receptor activity and ATP binding. KEGG pathway enrichment analysis displayed that DEmRNAs were markedly enriched in cell adhesion molecules, pathways in cancer, focal adhesion and phagosome (Figure 2B).

DEmiRNA-DEmRNA interaction network

DEmiRNA-DEmRNA interaction network analysis was performed for up-regulated and down-regulated miRNAs, respectively. For the up-regulated miRNAs, we obtained 397 DEmiRNA-DEmRNA pairs including 15 DEmiRNAs and 188 DEmRNAs. The DElncRNA-DEmRNA interaction network was consisted of 203 nodes and 397 edges (Fig. 3). Among the down-regulated miRNAs, a total of 937 DEmiRNAs-DEmRNAs pairs including 24 DEmiRNAs and 330 DEmRNAs were identified. The DElncRNA-DEmRNA interaction network consisted of 329 nodes and 937 edges (Fig. 4).

Functional enrichment analysis of DEmRNAs targeted by DEmiRNAs

As showed in Figure 5A, GO analysis results indicated that DEmRNAs targeted by DEmiRNAs were mainly enriched in signal transduction, multicellular organismal development and cell adhesion in the biological process. In the cellular component analysis, DEmRNAs targeted by DEmiRNAs were primarily enriched in the cytoplasm, integral to membrane and plasma membrane. In molecular function analysis, DEmRNAs targeted by DEmiRNAs were mainly enriched in protein binding, metal ion binding, nucleotide binding, receptor activity and ATP binding. KEGG pathway enrichment analysis displayed that DEmRNAs targeted by DEmiRNAs were markedly enriched in cell adhesion molecules, pathways in cancer, leukocyte transendothelial migration, cytokine-cytokine receptor interaction and MAPK signaling pathway (Fig. 5B).

Validation by QRT-PCR

To confirm the results of our integrated analysis, the expression of 3 mRNAs (IRF6, PTGER3 and NTRK2) and 3 miRNAs (hsa-miR-133b, hsa-miR-449a and hsa-miR-873-5p) were measured by quantitative real-time PCR in the blood sample of patients with endometriosis and normal controls. As showed in Figure 6, PTGER3 and NTRK2 were up-regulated and IRF6, hsa-miR-133b, hsa-miR-449a and hsa-miR-873-

5p were down-regulated in endometriosis compared with normal control. Except for hsa-miR-133b, QRT-PCR results of other mRNAs were consistent with those of the GEO analysis.

Expression validation and diagnostic analysis of DEmRNAs

GSE7305 and GSE23339 datasets of endometriosis were used for expression analysis of IRF6, PTGER3 and NTRK2 (Fig. 7). The result showed that IRF6 was significantly down-regulated, PTGER3 and NTRK2 were significantly up-regulated, which was in line with bioinformatics analysis. In addition, diagnostic analysis of IRF6, PTGER3 and NTRK2 was performed in the GSE23339 dataset (Fig. 8). The AUC value of IRF6, PTGER3 and NTRK2 was more than 0.8, which suggested that they had a potential diagnostic value.

Immune cell infiltration analysis in endometriosis

The CIBERSORT algorithm was used to estimate the burden of immune infiltration subtypes in the tissue of endometriosis (Fig. 9). The percentages of 22 kinds of immunocyte subtypes between ectopic endometria and eutopic endometria were detected. Interestingly, infiltration of macrophages M2 ($p = 1.3e-08$) was the most significantly increased, the infiltration of NK cells activated ($p = 3.8e-11$) was the most obviously reduced in ectopic endometria.

DISCUSSION

Endometriosis is a usual gynecological disease in women's reproductive stage, and is defined as the hormone-dependent abnormal growth of cells outside the uterus including ovary, peritoneum, intestines and vagina . A small number of endometriosis patients may lead to further tumor formation . Therefore, identification of DEmRNAs and DEmiRNAs is crucial for uncovering the pathogenesis of endometriosis.

In the current study, bioinformatics analysis was used to analyze the mRNA expression profile in the GSE11691, GSE25628, GSE86534 and GSE105764 datasets. 508 up-regulated and 327 down-regulated mRNAs were obtained. In addition,

GSE105765 dataset was utilized to identify DEmiRNAs with DESeq2 package in R, and 39 (15 up-regulated and 24 down-regulated) DEmiRNAs were identified in endometriosis, which were further used to build a DEmiRNA-DEmRNA interaction network. Finally, the expression of three mRNAs (IRF6, PTGER3 and NTRK2) and three miRNAs (hsa-miR-133b, hsa-miR-449a and hsa-miR-873-5p) were measured by QRT-PCR.

There is increasing evidence that the has-miR-449 is silenced or down-regulated in various tumor cells and plays vital roles in tumor cell proliferation, migration and invasion . Zhao et al. [6] have found that hsa-miR-449a is declined in patient with endometriosis. Mu et al. [12] have revealed that hsa-miR-449a may be one of mechanisms by which acupuncture therapy help promotes endometrium receptivity and prepare for in vitro fertilization and embryo transplantation. Given that endometriosis shares many common characteristics with malignant diseases, including invasion and migration, the low expression of hsa-miR-449a is likely to play a crucial role in the pathogenesis of endometriosis. Then, QRT-PCR confirmed that the expression level of hsa-miR-449a was significantly decreased in endometriosis and targeted prostaglandin-endoperoxidase synthase 3 (PTGER3). The expression level of PTGER3 is significantly increased in endometriosis . In this study, PTGER3 was up-regulated in both GEO integration analysis and QRT-PCR verification. Moreover, PTGER3 had a potential diagnostic value for endometriosis. Hence, we speculate that hsa-miR-449a-PTGER3 interaction is part of the pathogenesis of progression of endometriosis.

Hsa-miR-873 is observably down-regulated in ectopic pregnancy in viable intrauterine pregnancy and spontaneous abortion patients, and it is considered to be a valuable noninvasive and stable biomarker for early detection of ectopic pregnancy . In our study, hsa-miR-873-5p was reduced in both GSE105765 dataset and QRT-PCR verification. Neurotrophic receptor tyrosine kinase 2 (NTRK2) was targeted by hsa-miR-873-5p. NTRK2, a member of the tropomyosin receptor kinase family, has previously been associated with multiple cancers, including lung cancer, breast cancer

and pilocytic astrocytoma . Importantly, NTRK2 was up-regulated in both GEO integration analysis and QRT-PCR verification. Besides, KEGG pathway enrichment analysis found that NTRK2 was enriched in the MAPK pathway. It is noted that NTRK2 could be considered as a diagnostic biomarker for endometriosis. We infer that hsa-miR-873-5p-NTRK2 interaction plays a pivotal role in the development and progression of endometriosis by regulating MAPK pathway.

Hsa-miR-133b, located on chromosome 6p12.2, is highly expressed in muscle development and initially considered as a muscle-specific miRNA . Subsequent reports have shown that hsa-miR-133b can be widely detected in a variety of tissues. Xiao et al. [19] have found that hsa-miR-133b is up-regulated in oocytes treated with IGF-1 compared with the negative control, and hsa-miR-133b may play important roles in the growth and maturation of oocytes. In our study, hsa-miR-133b was elevated in endometrium and targeted interferon regulatory factor 6 (IRF6). IRF6 belongs to a family of nine transcription factors and has a highly conserved helix-Transshelix-helix DNA binding domain and a less conserved protein binding domain . IRF6 has been reported to be associated with endometriosis . Interesting, IRF6 was one of the top 10 DEmRNAs and down-regulated in both GEO integration analysis and QRT-PCR verification. In addition, IRF6 had a potential diagnostic value for endometriosis. These findings indicate that hsa-miR-133b-IRF6 may be involved in regulating the progression of endometriosis.

Endometriosis is a chronic inflammatory disease related to the impaired immune response at the site of lesion implantation . The abnormal distribution of immune cells has been found in the abdominal cavity of endometriosis patients . In this study, the CIBERSORT algorithm was used to estimate the burden of immune infiltration subtypes in the tissue of endometriosis. The percentages of 22 kinds of immunocyte subtypes between ectopic endometria and eutopic endometria were detected. We found that the infiltration of macrophages M2 was the most significantly increased, the infiltration of NK cells activated was the most obviously reduced in ectopic endometria. Macrophages belong to the mononuclear phagocyte system that is part of

both the innate immune system and the adaptive immune system . It is found that M2 macrophages are associated with resolution of inflammation and promotion of tissue repair . Previous report has confirmed that M2 macrophages infiltrates endometriotic lesions and promotes angiogenesis . In patients with endometriosis with pelvic pain, the proportion of NK cells in the peripheral blood is significantly higher than that of women with stable disease without pelvic pain . Suppressing the cytotoxic activity of NK cells may help to reduce the progression of pelvic pain in endometriosis patients. This suggested that macrophages M2 and NK cells activated may play an important role in endometriosis.

CONCLUSIONS

Based on integrated analysis, we obtained 835 DEmRNAs and 39 DEmiRNAs in endometriosis. In addition, a miRNA-mRNA interaction network was constructed to find the crucial DEmiRNA-DEmRNA pairs that play an important role in the pathogenesis of endometriosis. Moreover, key DEmiRNA-DEmRNA pairs were also verified using QRT-PCR. These identified DEmRNAs and DEmiRNAs may be involved in the pathogenesis of endometriosis. However, there are limitations to our study. Firstly, this study is only based on integrated analysis and QRT-PCR validation. Further large sample studies are needed to validate the expression of identified mRNAs and miRNAs in endometriosis. Secondly, some functional experiment is further needed to investigate the deeper molecular mechanism of identified mRNAs and miRNAs in endometriosis.

Availability of data and materials

The datasets used and analyzed during the current study are available from public database Gene Expression Omnibus repository. Accession numbers of the datasets used in this study are GSE11691, GSE25628, GSE86534 and GSE105764 in Gene Expression Omnibus (https://www.ncbi.nlm.nih.gov/geo).

Conflict of interest

The authors declare that they have no conflict of interest.

REFERENCES

1. Obrzut M, Obrzut B, Zmuda M, et al. Uterine leiomyomas: correlation between histologic composition and stiffness via magnetic resonance elastography - a Pilot Study. Ginekol Pol. 2020; 91(7): 373–378, doi: 10.5603/GP.a2020.0067, indexed in Pubmed: 32542642.
2. Liu F, Lv X, Yu H, et al. In search of key genes associated with endometriosis using bioinformatics approach. Eur J Obstet Gynecol Reprod Biol. 2015; 194: 119–124, doi: 10.1016/j.ejogrb.2015.08.028, indexed in Pubmed: 26366788.
3. Clough E, Barrett T. The gene expression omnibus database. Methods Mol Biol. 2016; 1418: 93–110, doi: 10.1007/978-1-4939-3578-9_5, indexed in Pubmed: 27008011.
4. Zhang Y, Ma L. Identification of key genes and pathways in calcific aortic valve disease by bioinformatics analysis. J Thorac Dis. 2019; 11(12): 5417–5426, doi: 10.21037/jtd.2019.11.57, indexed in Pubmed: 32030260.
5. Rung J, Brazma A. Reuse of public genome-wide gene expression data. Nat Rev Genet. 2013; 14(2): 89–99, doi: 10.1038/nrg3394, indexed in Pubmed: 23269463.
6. Zhao L, Gu C, Ye M, et al. Integration analysis of microRNA and mRNA paired expression profiling identifies deregulated microRNA-transcription factor-gene regulatory networks in ovarian endometriosis. Reprod Biol Endocrinol. 2018; 16(1): 4, doi: 10.1186/s12958-017-0319-5, indexed in Pubmed: 29357938.
7. Qi H, Liang G, Yu J, et al. Genome-wide profiling of miRNA expression patterns in tubal endometriosis. Reproduction. 2019; 157(6): 525–534, doi: 10.1530/REP-18-0631, indexed in Pubmed: 30909166.
8. Baranov VS, Ivaschenko TE, Liehr T, et al. Systems genetics view of endometriosis: a common complex disorder. Eur J Obstet Gynecol Reprod

Biol. 2015; 185: 59–65, doi: 10.1016/j.ejogrb.2014.11.036, indexed in Pubmed: 25528731.

9. Aznaurova YB, Zhumataev MB, Roberts TK, et al. Molecular aspects of endometriosis. Reprod Biol Endocrinol. 2015; 12: 50, doi: 10.1186/1477-7827-12-50, indexed in Pubmed: 24927773.
10. Kheir TB, Futoma-Kazmierczak E, Jacobsen A, et al. miR-449 inhibits cell proliferation and is down-regulated in gastric cancer. Mol Cancer. 2011; 10: 29, doi: 10.1186/1476-4598-10-29, indexed in Pubmed: 21418558.
11. Sandbothe M, Buurman R, Reich N, et al. The microRNA-449 family inhibits TGF-β-mediated liver cancer cell migration by targeting SOX4. J Hepatol. 2017; 66(5): 1012–1021, doi: 10.1016/j.jhep.2017.01.004, indexed in Pubmed: 28088579.
12. Mu Y, Li Q, Cheng J, et al. Integrated miRNA-seq analysis reveals the molecular mechanism underlying the effect of acupuncture on endometrial receptivity in patients undergoing fertilization: embryo transplantation. 3 Biotech. 2020; 10(1): 6, doi: 10.1007/s13205-019-1990-3, indexed in Pubmed: 31824817.
13. Santulli P, Borghese B, Noël JC, et al. Hormonal therapy deregulates prostaglandin-endoperoxidase synthase 2 (PTGS2) expression in endometriotic tissues. J Clin Endocrinol Metab. 2014; 99(3): 881–890, doi: 10.1210/jc.2013-2950, indexed in Pubmed: 24423291.
14. Lu Qi, Yan Qi, Xu F, et al. MicroRNA-873 is a Potential Serum Biomarker for the Detection of Ectopic Pregnancy. Cell Physiol Biochem. 2017; 41(6): 2513–2522, doi: 10.1159/000475946, indexed in Pubmed: 28472791.
15. Wang X, Xu Z, Chen Xi, et al. A tropomyosin receptor kinase family protein, NTRK2 is a potential predictive biomarker for lung adenocarcinoma. PeerJ. 2019; 7: e7125, doi: 10.7717/peerj.7125, indexed in Pubmed: 31245181.
16. Wang JJ, Huang YQ, Song W, et al. Comprehensive analysis of the lncRNA-associated competing endogenous RNA network in breast cancer.

Oncol Rep. 2019; 42(6): 2572–2582, doi: 10.3892/or.2019.7374, indexed in Pubmed: 31638237.

17. Pattwell SS, Konnick EQ, Liu YJ, et al. Neurotrophic receptor tyrosine kinase 2 (NTRK2) alterations in low-grade gliomas: report of a novel gene fusion partner in a pilocytic astrocytoma and review of the literature. Case Rep Pathol. 2020; 2020: 5903863, doi: 10.1155/2020/5903863, indexed in Pubmed: 32082673.
18. Panguluri SK, Bhatnagar S, Kumar A, et al. Genomic profiling of messenger RNAs and microRNAs reveals potential mechanisms of TWEAK-induced skeletal muscle wasting in mice. PLoS One. 2010; 5(1): e8760, doi: 10.1371/journal.pone.0008760, indexed in Pubmed: 20098732.
19. Xiao G, Xia C, Yang J, et al. MiR-133b regulates the expression of the Actin protein TAGLN2 during oocyte growth and maturation: a potential target for infertility therapy. PLoS One. 2014; 9(6): e100751, doi: 10.1371/journal.pone.0100751, indexed in Pubmed: 24959893.
20. Xu L, Huang TJ, Hu H, et al. The developmental transcription factor IRF6 attenuates ABCG2 gene expression and distinctively reverses stemness phenotype in nasopharyngeal carcinoma. Cancer Lett. 2018; 431: 230–243, doi: 10.1016/j.canlet.2017.10.016, indexed in Pubmed: 29111349.
21. Bhyan SB, Zhao Li, Wee Y, et al. Genetic links between endometriosis and cancers in women. PeerJ. 2019; 7: e8135, doi: 10.7717/peerj.8135, indexed in Pubmed: 31879572.
22. Lousse JC, van Langendonckt A, Defrere S, et al. Peritoneal endometriosis is an inflammatory disease. Frontiers in Bioscience. 2012; 4(1): 23–40, doi: 10.2741/358, indexed in Pubmed: 22201853.
23. Braun DP, Dmowski WP. Endometriosis: abnormal endometrium and dysfunctional immune response. Curr Opin Obstet Gynecol. 1998; 10(5): 365–369, doi: 10.1097/00001703-199810000-00003, indexed in Pubmed: 9818213.
24. Jones RK, Bulmer JN, Searle RF. Phenotypic and functional studies of leukocytes in human endometrium and endometriosis. Hum Reprod Update.

1998; 4(5): 702–709, doi: 10.1093/humupd/4.5.702, indexed in Pubmed: 10027623.

25. Hume DA. The mononuclear phagocyte system. Curr Opin Immunol. 2006; 18(1): 49–53, doi: 10.1016/j.coi.2005.11.008, indexed in Pubmed: 16338128.
26. Mantovani A, Sica A, Sozzani S, et al. The chemokine system in diverse forms of macrophage activation and polarization. Trends Immunol. 2004; 25(12): 677–686, doi: 10.1016/j.it.2004.09.015, indexed in Pubmed: 15530839.
27. Bacci M, Capobianco A, Monno A, et al. Macrophages are alternatively activated in patients with endometriosis and required for growth and vascularization of lesions in a mouse model of disease. Am J Pathol. 2009; 175(2): 547–556, doi: 10.2353/ajpath.2009.081011, indexed in Pubmed: 19574425.
28. Capobianco A, Monno A, Cottone L, et al. Proangiogenic Tie2(+) macrophages infiltrate human and murine endometriotic lesions and dictate their growth in a mouse model of the disease. Am J Pathol. 2011; 179(5): 2651–2659, doi: 10.1016/j.ajpath.2011.07.029, indexed in Pubmed: 21924227.
29. He J, Xu Y, Yi M, et al. Involvement of natural killer cells in the pathogenesis of endometriosis in patients with pelvic pain. J Int Med Res. 2020; 48(7): 300060519871407, doi: 10.1177/0300060519871407, indexed in Pubmed: 32727237.

Table 1. Details of GEO endometriosis data

GEO ID	Samples (EU:EC)	Type	Platform	Year	Author	Type
GSE11691	7:9	mRNA	GPL96	2008	D.Stephen Charnock-Jones	Tissue
GSE25628	7:6	mRNA	GPL571	2013	Raffaele A Calogero	Tissue
GSE86534	4:4	mRNA	GPL20115	2019	Chen Zhang	Tissue
GSE105764	8:8	mRNA	GPL20301	2018	Luyang Zhao	Tissue
GSE105764	8:8	miRNA	GPL11154	2018	Luyang Zhao	Tissue

5

E — eutopic endometrial; EC — ectopic endometrial

Table 2. The top 10 up- and down-regulated DEmRNAs

ID	Symbol	Combined.ES	P value	FDR	Up/Down
165	AEBP1	5.167795	0	0	Up
185	AGTR1	3.486139	0	0	Up
358	AQP1	3.694497	0	0	Up
633	BGN	3.555798	0	0	Up
684	BST2	3.953571	0	0	Up
730	C7	5.401551	0	0	Up
1296	COL8A2	5.345685	0	0	Up
1359	CPA3	3.413792	0	0	Up
1475	CSTA	4.274204	0	0	Up
1809	DPYSL3	4.468443	0	0	Up
1832	DSP	–3.70545	0	0	Down
3216	HOXB6	–4.9245	0	0	Down
3664	IRF6	–4.44489	0	0	Down
5357	PLS1	–3.57045	0	0	Down
5774	PTPN3	–4.15988	0	0	Down
7163	TPD52	–3.42889	0	0	Down
7368	UGT8	–3.97117	0	0	Down
9053	MAP7	–4.37345	0	0	Down
10053	AP1M2	–3.80742	0	0	Down
10653	SPINT2	–3.57607	0	0	Down

ES — effect size; FDR — false discovery rate

Table 3. All DEmiRNA between EC and EU

Symbol	Base mean	Log_2FC	P value	FDR	Up/Down
hsa-miR-449b-5p	1086.373	–6.97688	1.76E-52	1.07E-49	Down
hsa-miR-141-3p	86518.7	–6.10501	4.94E-44	1.09E-41	Down
hsa-miR-202-5p	2763.408	9.463128	5.37E-44	1.09E-41	Up
hsa-miR-34c-3p	107.9907	–4.91143	2.73E-39	4.15E-37	Down
hsa-miR-34b-5p	1164.497	–5.14853	1.62E-38	1.64E-36	Down
hsa-miR-200c-3p	6715.331	–4.8971	1.50E-38	1.64E-36	Down
hsa-miR-375-3p	9495.127	–7.56061	3.29E-36	2.86E-34	Down
hsa-miR-449a	2592.821	–6.34734	3.65E-35	2.78E-33	Down
hsa-miR-708-5p	5194.45	3.202732	5.47E-35	3.69E-33	Up
hsa-miR-200a-3p	5035.966	–5.29445	7.57E-35	4.60E-33	Down
hsa-miR-141-5p	623.3556	–5.33507	1.31E-34	7.23E-33	Down
hsa-miR-449c-5p	2901.445	–6.88749	2.80E-34	1.42E-32	Down
hsa-miR-34c-5p	8806.229	–4.67436	4.91E-31	2.30E-29	Down
hsa-miR-196b-3p	43.35577	–3.92688	4.16E-29	1.81E-27	Down
hsa-miR-200b-5p	259.7849	–4.57665	7.06E-27	2.68E-25	Down
hsa-miR-200a-5p	240.5646	–4.72025	1.53E-26	5.47E-25	Down
hsa-miR-34b-3p	134.4835	–4.1418	4.63E-21	1.57E-19	Down
hsa-miR-216a-5p	33.17238	4.37693	1.56E-20	5.00E-19	Up
hsa-miR-10a-5p	233418.6	–3.43782	1.26E-19	3.84E-18	Down
hsa-miR-196b-5p	11000.64	–4.02737	1.49E-19	4.31E-18	Down
hsa-miR-675-3p	162.5129	–3.12799	2.13E-19	5.62E-18	Down
hsa-miR-10a-3p	778.103	–3.5977	1.10E-18	2.56E-17	Down
hsa-miR-223-3p	2210.115	3.033881	4.21E-17	8.53E-16	Up
hsa-miR-217-5p	52.13757	4.165841	6.62E-17	1.30E-15	Up
hsa-miR-200b-3p	6496.317	–4.06437	5.63E-16	1.04E-14	Down
hsa-miR-514a-3p	250.334	6.071821	1.92E-14	3.08E-13	Up
hsa-miR-187-3p	189.1282	–4.31383	5.58E-13	7.89E-12	Down
hsa-miR-615-3p	117.1398	3.897824	2.16E-12	2.79E-11	Up
hsa-miR-509-3p	1752.883	6.502398	2.30E-12	2.91E-11	Up
hsa-miR-133b	15.98328	3.316177	3.28E-12	4.06E-11	Up
hsa-miR-203a-3p	1936.05	–3.40336	1.27E-11	1.49E-10	Down
hsa-miR-513c-5p	103.668	6.525797	3.85E-10	3.77E-09	Up
hsa-miR-7974	13.6423	–3.3685	5.38E-09	4.36E-08	Down
hsa-miR-508-5p	33.38197	5.767593	7.19E-08	4.86E-07	Up
hsa-miR-873-5p	167.9197	–3.52944	1.27E-07	8.04E-07	Down
hsa-miR-506-3p	24.203	4.292988	2.11E-07	1.26E-06	Up
hsa-miR-509-5p	30.98636	4.127607	3.95E-07	2.19E-06	Up
hsa-miR-513b-5p	38.95121	5.924017	6.81E-07	3.67E-06	Up
hsa-miR-137-3p	20.66388	3.527503	1.60E-05	7.01E-05	Up

FC — fold change; FDR — false discovery rate

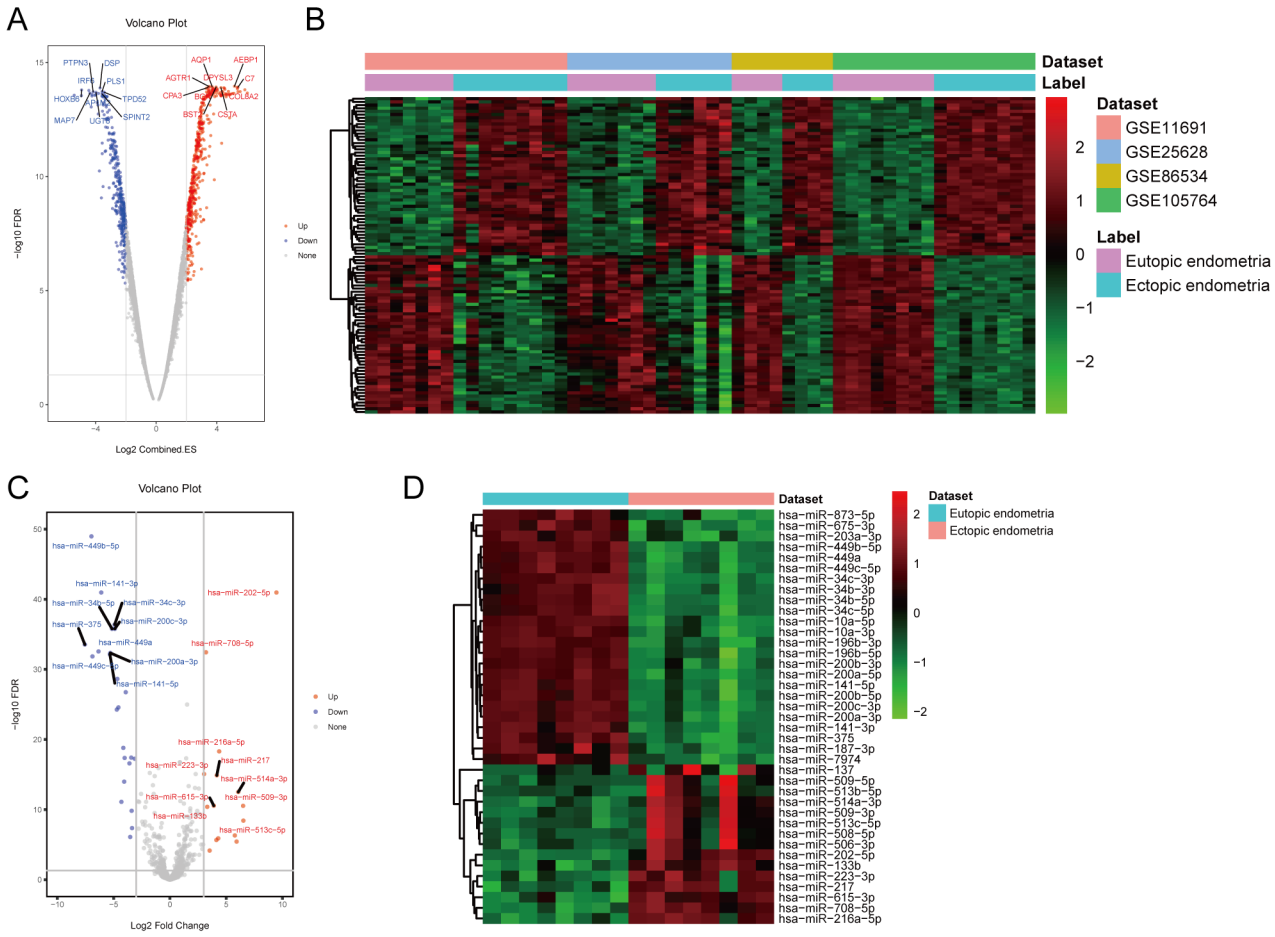

Figure 1. DEmRNA and DEmiRNA between EC and EU. **A.** The volcano plot of DEmRNAs; **B.** The heatmap of top 100 DEmRNAs. Rows and columns represent DEmRNAs and tissue samples, respectively. Red and green color were used to represent up- and downregulation, respectively; **C.** The volcano plot of DEmiRNAs; **D.** The heatmap of all DEmiRNAs. Rows and columns represent DEmRNAs and tissue samples, respectively. Red and green color is used to represent up- and downregulation, respectively

Figure 2A

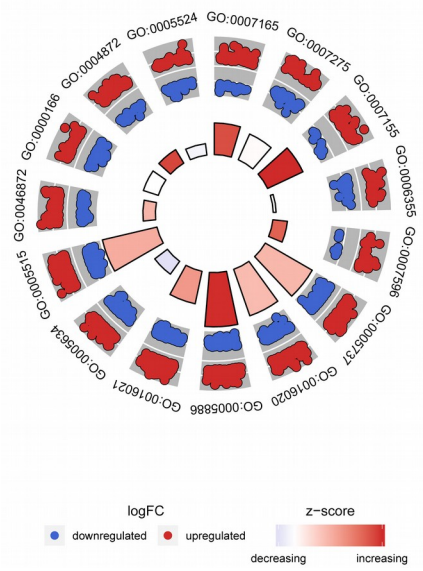

ID	Description
GO:0007165	signal transduction (BP)
GO:0007275	multicellular organismal development (BP)
GO:0007155	cell adhesion (BP)
GO:0006355	regulation of transcription, DNA−dependent (BP)
GO:0007596	blood coagulation (BP)
GO:0005737	cytoplasm (CC)
GO:0016020	membrane (CC)
GO:0005886	plasma membrane (CC)
GO:0016021	integral to membrane (CC)
GO:0005634	nucleus (CC)
GO:0005515	protein binding (MF)
GO:0046872	metal ion binding (MF)
GO:0000166	nucleotide binding (MF)
GO:0004872	receptor activity (MF)
GO:0005524	ATP binding (MF)

Figure 2B

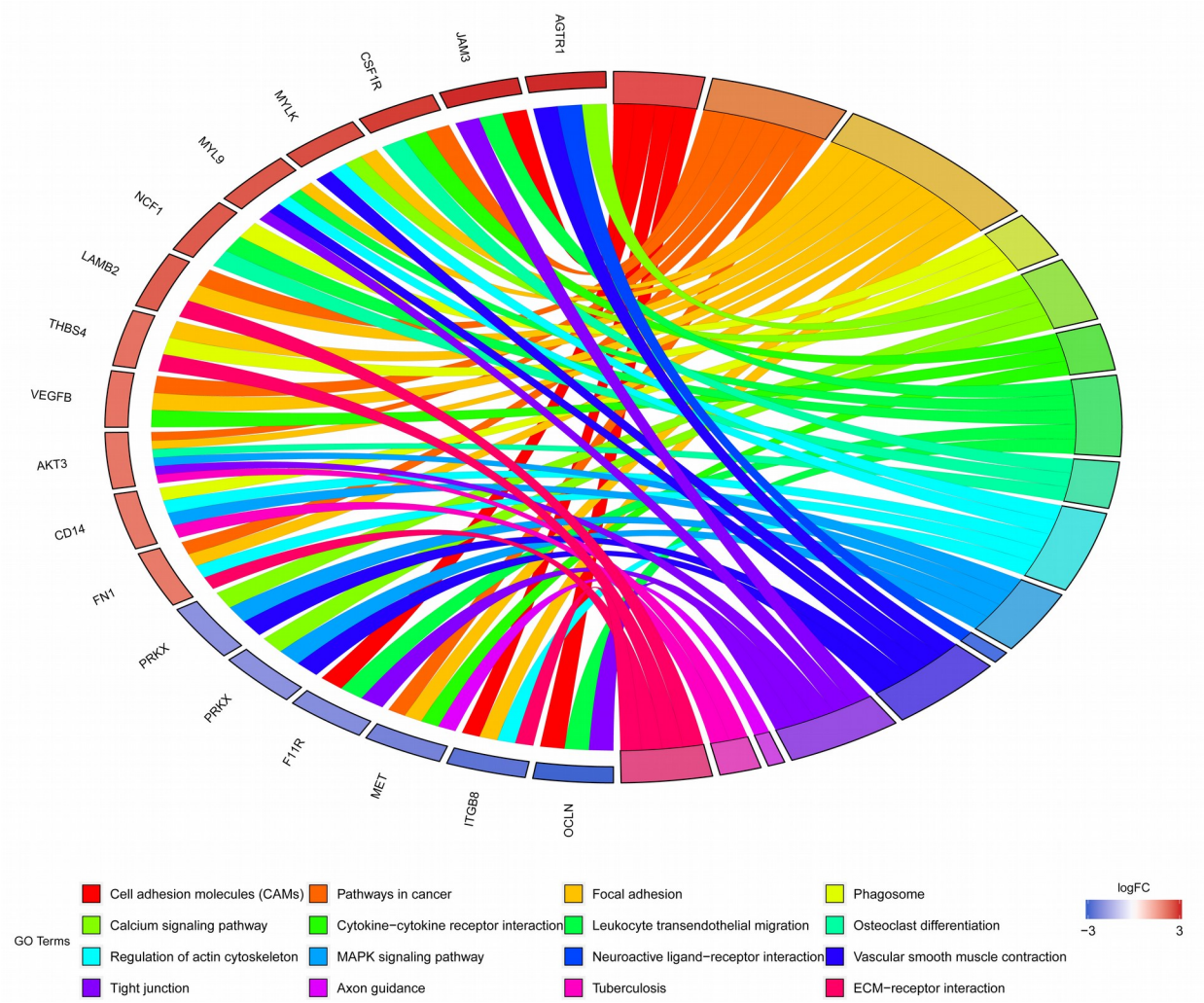

Figure 2. Functional enrichment analysis of DEmRNAs. **A.** GO enrichment analyses of DEmRNAs; **B.** KEGG pathway enrichment analyses of DEmRNAs

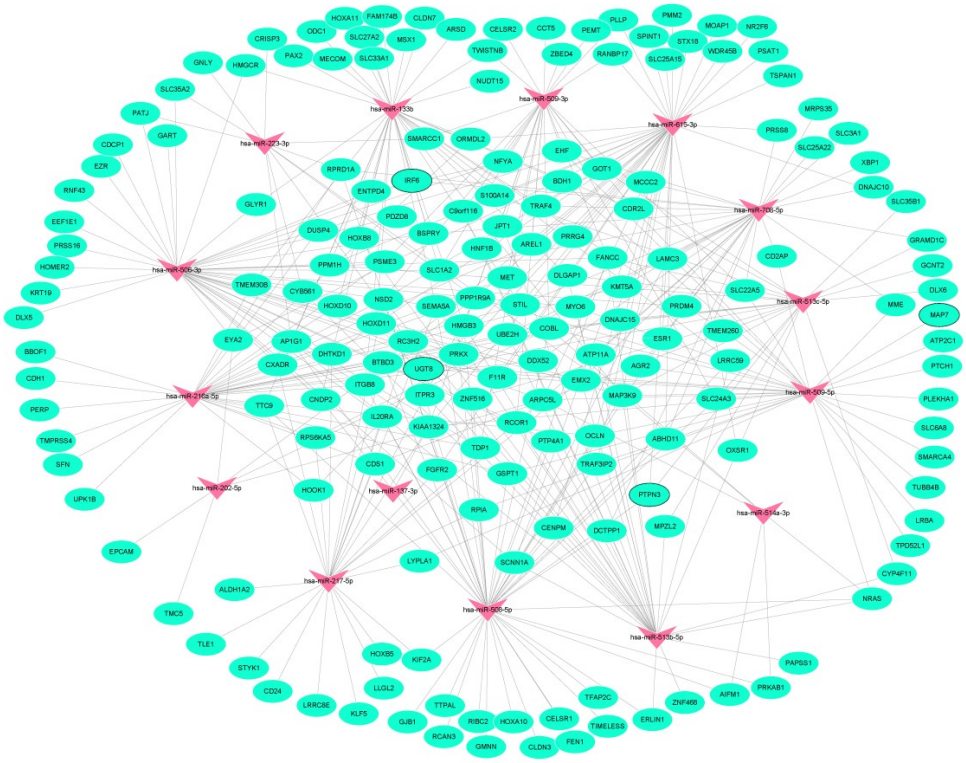

Figure 3. DEmiRNA-DEmRNA interaction network of up-regulated DEmiRNAs. The inverted triangles and ellipses represent the DEmiRNAs and DEmRNA, respectively. Red and green color represents up- and down-regulation, respectively

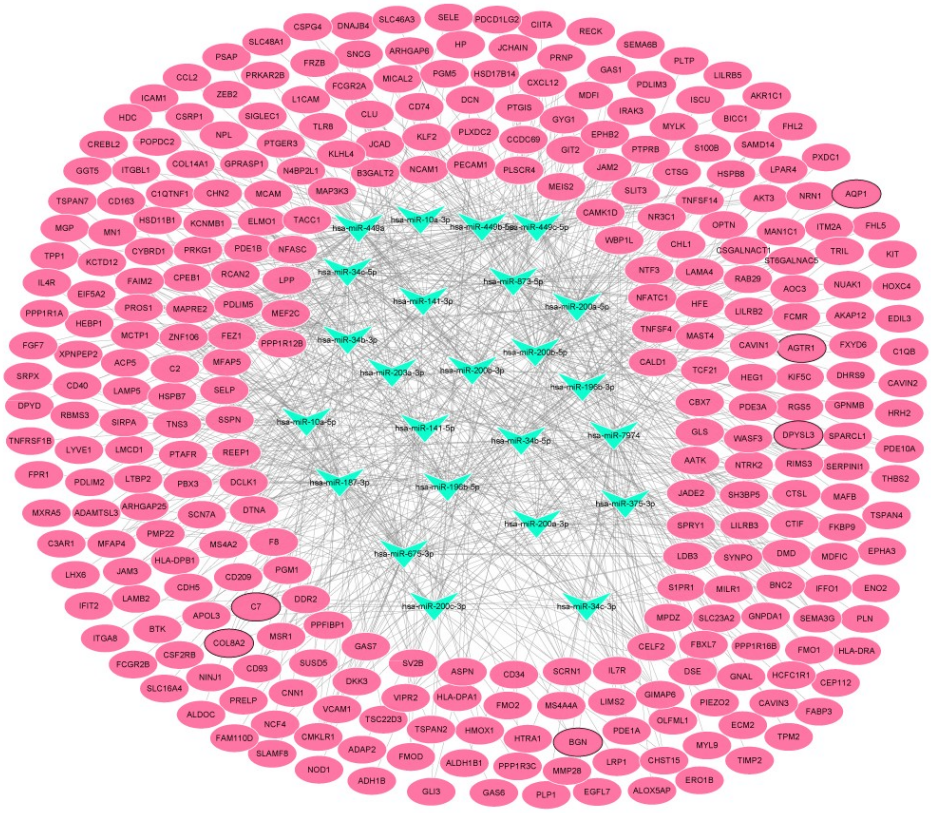

Figure 4. DEmiRNA-DEmRNA interaction network of down-regulated DEmiRNAs. The inverted triangles and ellipses represent the DEmiRNAs and DEmRNA, respectively. Red and green color represents up- and down-regulation, respectively

Figure 5A

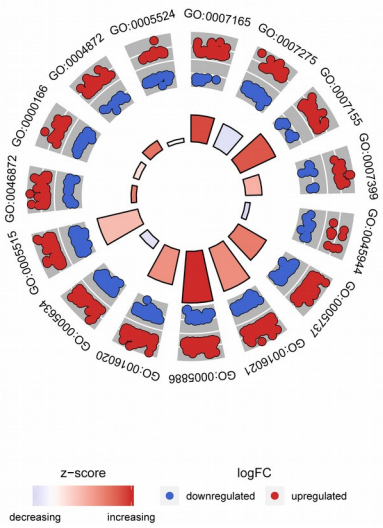

ID	Description
GO:0007165	signal transduction (BP)
GO:0007275	multicellular organismal development (BP)
GO:0007155	cell adhesion (BP)
GO:0007399	nervous system development (BP)
GO:0045944	positive regulation of transcription from RNA polymerase II promoter (BP)
GO:0005737	cytoplasm (CC)
GO:0016021	integral to membrane (CC)
GO:0005886	plasma membrane (CC)
GO:0016020	membrane (CC)
GO:0005634	nucleus (CC)
GO:0005515	protein binding (MF)
GO:0046872	metal ion binding (MF)
GO:0000166	nucleotide binding (MF)
GO:0004872	receptor activity (MF)
GO:0005524	ATP binding (MF)

Figure 5B

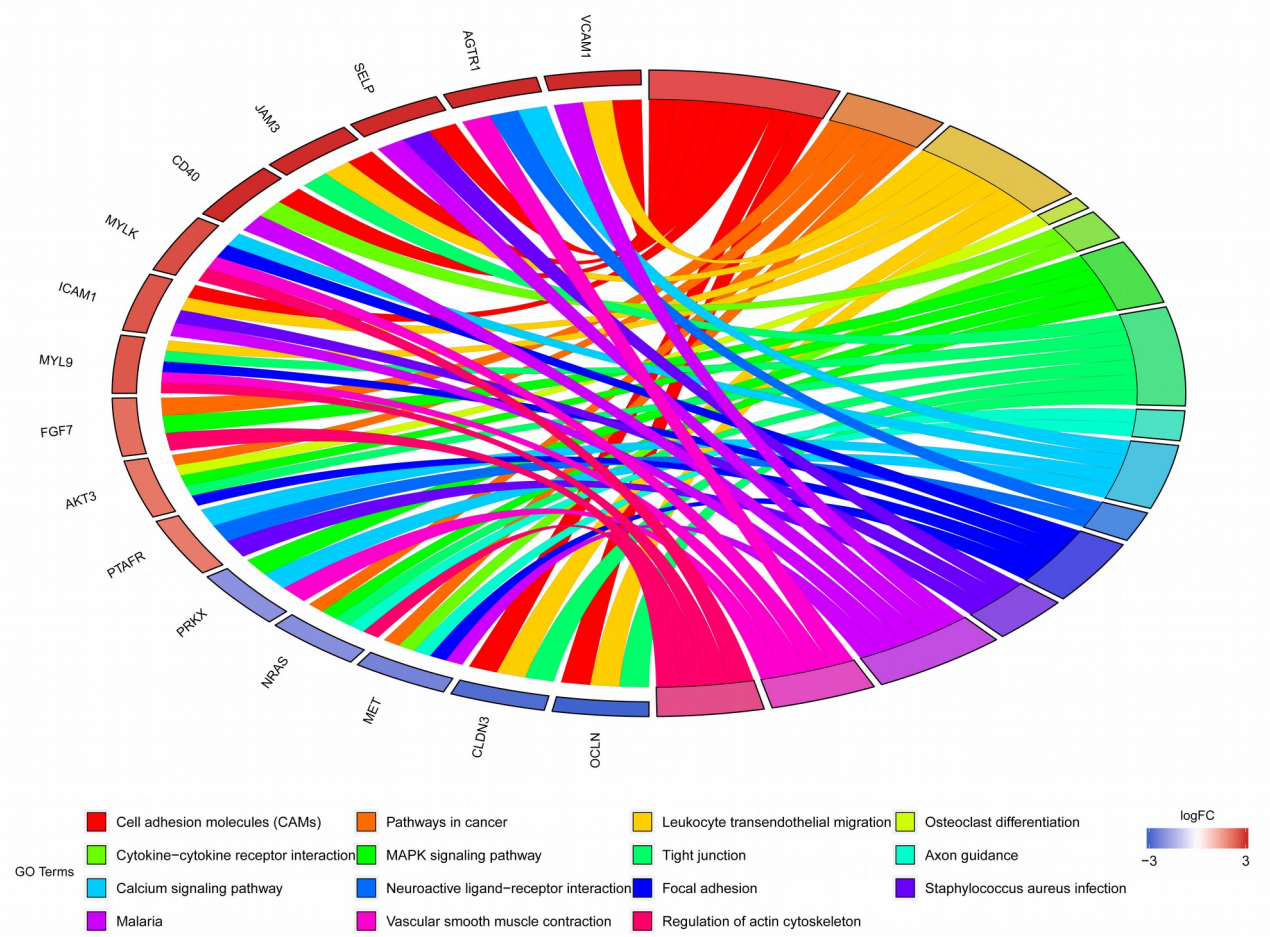

Figure 5. Functional enrichment analysis of DEmRNAs. **A.** GO enrichment analyses of DEmRNAs; **B.** KEGG pathway enrichment analyses of DEmRNAs

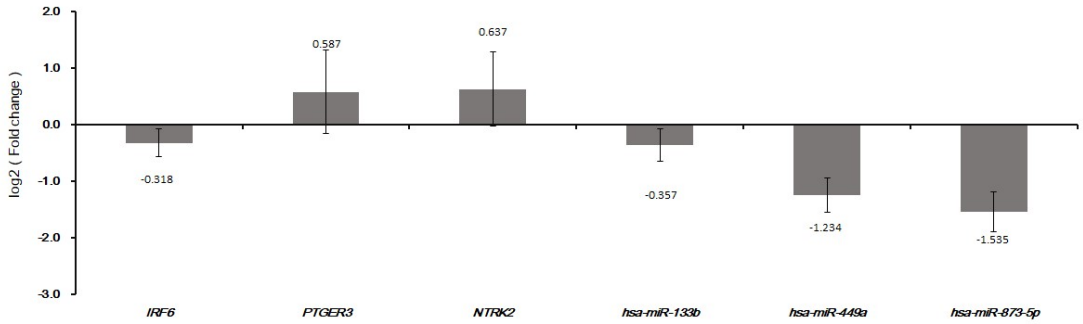

Figure 6. Validation of DEmRNA and DEmiRNA by QRT-PCR. The expression of DEmRNA and DEmiRNA was detected by QRT-PCR assay. All assays were performed three times independently at least

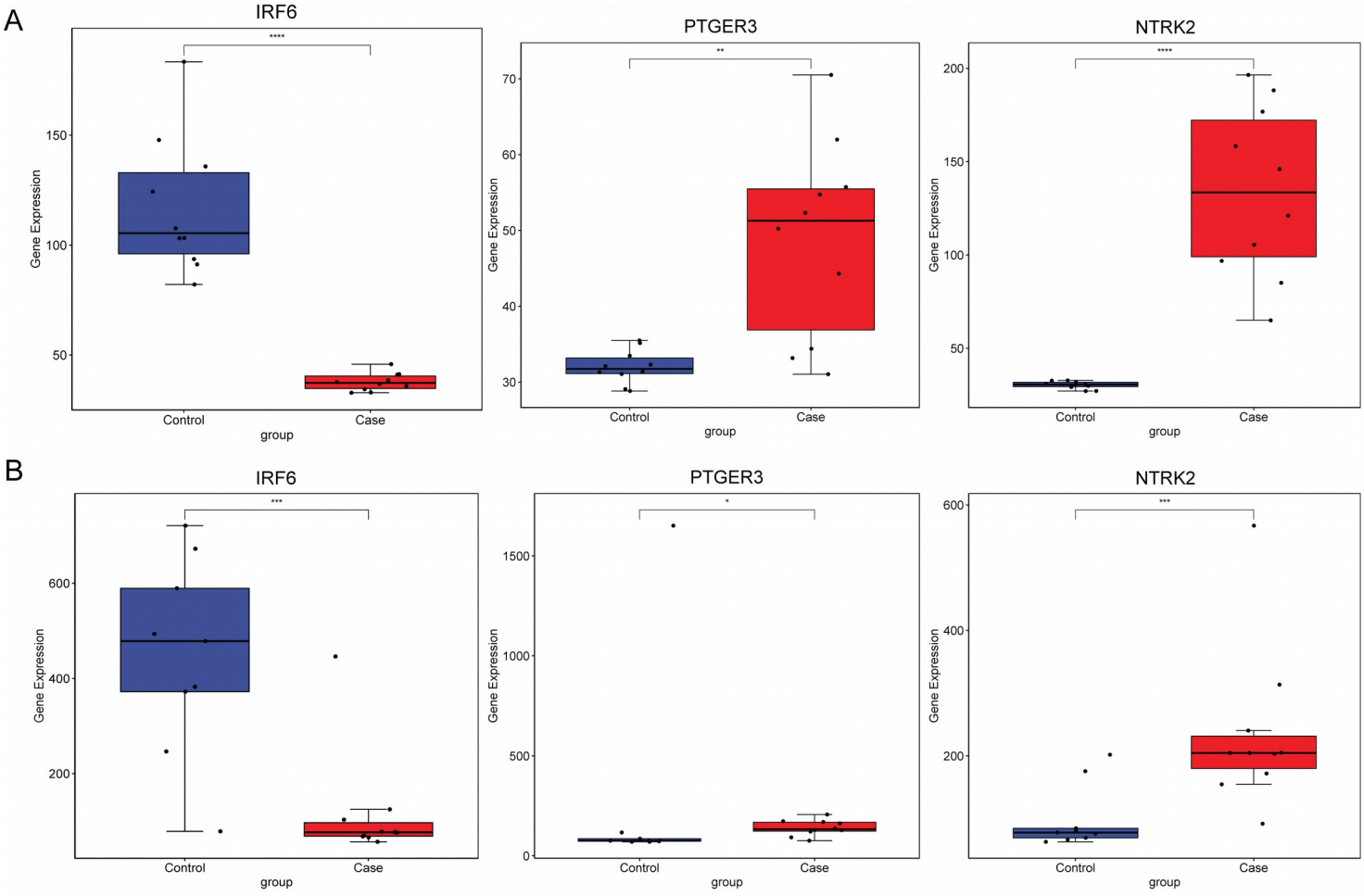

*p < 0.05; **p < 0.01; ***p < 0.001; ****p < 0.0001

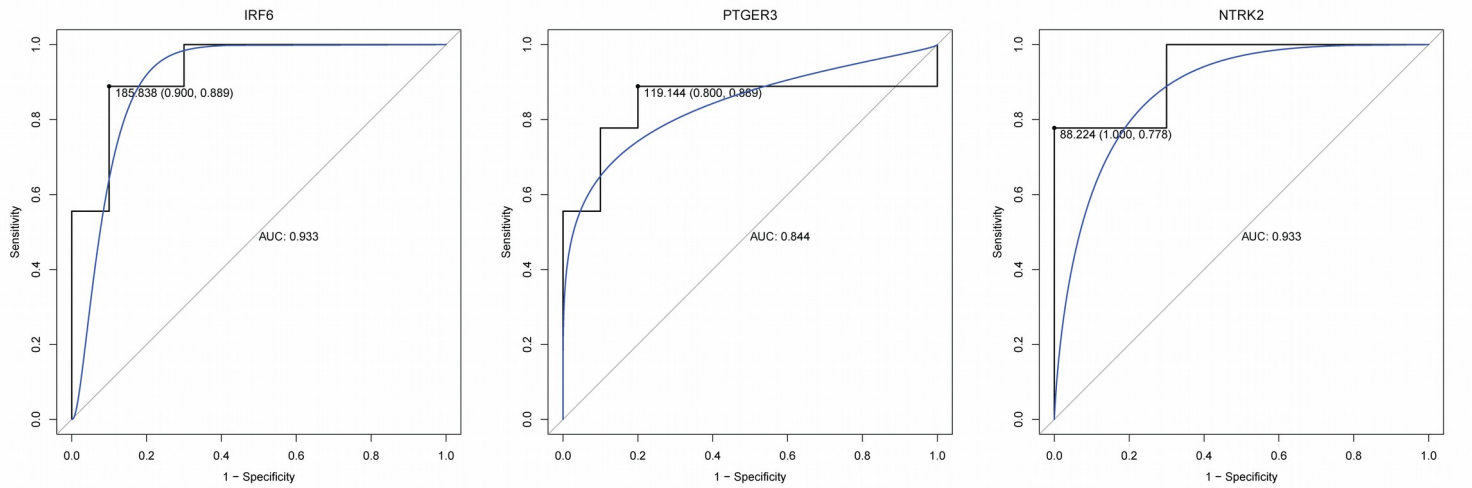

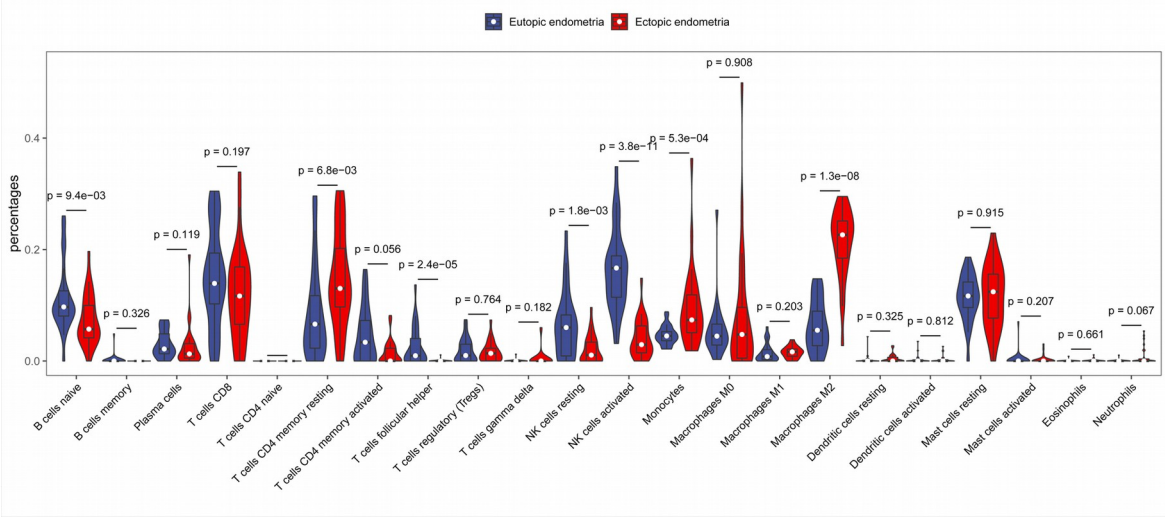

endometria and eutopic endometria